Available online at www.sciencedirect.com
ScienceDirect
Journal of Power Sources 178 (2008) 510–516
JOURNAL OF POWER SOURCES
www.elsevier.com/locate/jpowsour

Non-precious metal oxygen reduction catalyst for PEM fuel cells based on nitroaniline precursor☆

Thomas E. Wood[a,*], Zhongshu Tan[a], Alison K. Schmoeckel[b], David O'Neill[c], Radoslav Atanasoski[b,**]

[a] Central Research Materials Laboratory, 3M Company, 3M Center, 0201-02-S-05, St. Paul, MN 55144-1000, USA
[b] Fuel Cell Program, 3M Company, 3M Center, 0201-02-S-05, St. Paul, MN 55144-1000, USA
[c] Central Research Process Laboratory, 3M Company, 3M Center, 0201-02-S-05, St. Paul, MN 55144-1000, USA

Received 24 October 2007; accepted 26 October 2007
Available online 17 November 2007

Abstract

The cost of platinum is one of the major obstacles in the commercialization of proton exchange membrane fuel cells. Non-precious metal catalysts (NPMC) as an inexpensive substitute for platinum have been viewed as the only long-term solution to the problem. In this paper, we introduce new precursors used to synthesize NPMC active sites through metal-assisted polymerization of nitrogen-containing, aromatic molecules. Results of electrochemical characterization, which was performed in a real fuel cell environment, with emphasis on the activity of the catalyst are presented. Catalytic activity among the highest in the NPMC area was obtained when using 4-nitroaniline as a precursor.

Keywords: Fuel cell; Non-precious metal; Catalyst; Oxygen reduction; Polymer precursor

1. Introduction

Replacing platinum as a catalyst in hydrogen–air fuel cells, particularly in proton exchange membrane (PEM) fuel cells (FC), has long been an industry goal. Well-known drawbacks of using platinum as a catalyst are its price and scarcity. An additional, fundamental limitation is that the use of platinum makes the fuel cell operation energy inefficient. At high voltages platinum reacts with water and oxygen [1,2] producing a surface oxide layer that inhibits catalysis of the oxygen reduction reaction (ORR). To compensate for this drawback, much higher loadings of platinum are needed on the cathode side, where the reduction of oxygen (from air) takes place. With this consideration, developing a suitable replacement for platinum as a catalyst for the ORR could contribute significantly to fuel cells becoming commercially viable.

From an application point of view, a successful PEM fuel cell catalyst should satisfy three essential requirements: performance, durability and cost. This report will focus on the performance of a non-precious metal catalyst (NPMC) based on nitroaniline precursors. Catalyst performance is determined by the site-specific catalytic activity for ORR and by the surface density of these active catalyst centers at the catalyst–membrane (electrolyte) interface. For platinum, every surface platinum atom is potentially a catalytically active site. In the case of non-precious metal catalysts, the catalytic sites of interest are believed to be multi-atomic entities rather than single atoms, the structure of which is not certain. This implies that the surface packing density of multi-atomic catalytic centers will play a crucial role in the total activity of NPMCs.

Numerous articles have been published discussing ORR catalysis by transition metal compounds, including an excellent review by Dodelet [3] where both the developments leading to and the work most relevant to our own approach are summarized in a comprehensive way. In the last several years, Dodelet's group produced time-of-flight secondary ion mass spectroscopy (SIMS) data and X-ray photoelectron spectroscopy (XPS) spectra from which they proposed that the composition of the most catalytically active functional group is Fe–N_2–C_x [4]. The two

☆ Based on invited talk at the "Polymer Batteries—Fuel Cells, PBFC, 2007" International Conference, Rome, June 2007.

* Corresponding author. Tel.: +1 651 736 0820; fax: +1 651 737 4682.
** Corresponding author. Tel.: +1 651 733 9441; fax: +1 651 575 1187.
E-mail addresses: tewood2@mmm.com (T.E. Wood), rtatanasoski@mmm.com (R. Atanasoski).

0378-7753/$ – see front matter © 2007 Elsevier B.V. All rights reserved.
doi:10.1016/j.jpowsour.2007.10.093

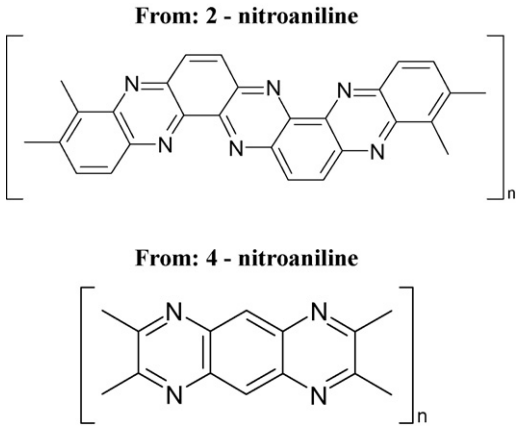

Fig. 1. Possible polymer structures derived from 2-nitroaniline (upper) and 4-nitroaniline (lower). Note that the nitrogen in the quinoxaline repeating subunits is pyrazinic rather than pyridinic.

nitrogen atoms to which iron is coordinated are claimed to be pyridinic in nature and can be either in a phenanthroline configuration or can be located at the edges of the opposite walls of the carbon micropores [5]. Based on their model, Dodelet's group has postulated that the key to achieving higher activity is to increase the amount of nitrogen-coordinated iron by first increasing the surface concentration of pyridinic nitrogen.

3M approach. As part of a broader effort to develop more efficient NPMC for ORR, we adopted three strategic directions. One approach is based on vacuum deposition processes [6–8], the second approach is focused on synthesis of metal-containing nanoparticles finely dispersed on carbon substrates [9], and the third approach generates active sites through metal-assisted polymerization of nitrogen-containing aromatic molecules [10]. In this paper we present the results of the third approach where nitroaniline is used as the nitrogen-rich aromatic precursor molecule. Nitroaniline is part of a general class of materials that was developed at 3M as sorbents and oxidation catalysts by Errede et al. [11] and to our knowledge it has not been previously used as a precursor for ORR catalysts. Based on the reaction mechanism of the polymerization process, possible structures of the polymers derived from nitroaniline are depicted in Fig. 1. Note in Fig. 1 that the repeating subunits in the polymers are quinoxaline containing pyrazinic rather than pyridinic nitrogen.

We discovered that the polymerization of nitroaniline in combination with certain anhydrous metal salts, followed by a thermal treatment could be used to create NPMCs with greater activity than obtained with other precursor materials. While the details of the synthesis are given in Section 2, the three basic process steps can be described as follows:

1. The transition metal (iron) is intimately mixed with the monomer during polymerization.
2. The product is pyrolized at 800–1000 °C in a nitrogen-containing atmosphere to develop active sites.
3. The leachable metal is removed in an acid bath.

Dozens of catalyst samples derived from the nitroaniline precursor have been synthesized and tested. This paper presents examples of the electrochemical results measured on these materials. A unique aspect of our work is that all catalysts are tested by incorporation into a 50-cm^2 PEM fuel cell, which is considered the smallest size acceptable for reliable projections of activity in full size fuel cell stacks. Since this is application driven research, the catalytic activity results are also presented in a form convenient for automotive use, volumetric current densities [12]. The measured volumetric current densities are compared to the US Department of Energy (DOE) goals [13].

2. Experimental

2.1. Catalyst synthesis

The catalyst preparation consists of four to five major steps:

(a) mixing and heating the nitroaniline and the iron salt under an inert atmosphere to form a metal-containing polymer in the presence of carbon;
(b) activating the metal-containing polymer by firing in the presence of ammonia to form a metal-containing fuel cell cathode catalyst;
(c) milling the catalyst to maximize surface area;
(d) optionally, repeating the firing, step (b), after milling;
(e) washing the metal-containing fuel cell cathode catalyst with an acid to remove the leachable metal.

In a typical preparation, the anhydrous metal salt (generally an iron chloride) is mixed with nitroaniline in a molar ratio of ∼1:4 as dry powders, sometimes with additional metal salts or organic additives. Substrate material, e.g., finely divided carbon is blended into the dry mixture. This mixture is milled to a consistent color. The mixture is transferred to a thick-walled glass vessel fitted with gas inlet and outlet. The vessel is first purged with nitrogen, and then with nitrogen flowing, the dry mixture is heated to 150–170 °C while being stirred allowing the nitroaniline to melt and further homogenizing the reagents. The mixture is heated to slightly above 200 °C at which point it begins to polymerize with evolution of gas. After the gas evolution subsides, the mixture is heated to ∼300 °C to ensure complete polymerization.

The active catalyst is formed from the polymerized mixture in a tube furnace under flowing nitrogen (75%)–ammonia (25%) gas mixture at 800–1000 °C. The catalyst is ball-milled to break apart agglomerates formed during the thermal processing and to comminute the catalyst. The milled catalyst is then acid washed (2 M sulfuric acid) to remove the leachable portion of transition metals.

The results presented here were all obtained on catalysts deposited on Cabot C55 carbon powder (Cabot Corporation; surface area ∼55 m^2 g^{-1}). Cabot's C55 carbon is chosen on the basis of its enhanced electrochemical stability relative to other higher surface area carbons.

2.2. Catalyst ink, MEA and FC assembly

A dispersion of the catalyst particles is prepared by mixing approximately 10 g of 10–13% (by weight) aqueous Nafion® dispersion with 1.5–2.5 g of the catalyst particles and approximately 10 g of deionized water. The catalyst ink dispersion is hand-brushed onto a 50-cm^2 coupon of a carbon-paper support which is previously treated for hydrophobicity and coated with a gas diffusion microlayer. The catalyst loading on the final catalyst-coated-backing (CCB) is approximately 1 mg cm^{-2}. The CCB is vacuum-dried at 110 °C for ~20 min. The CCB serves as the cathode catalyst and gas diffusion layer (GDL) of the test membrane electrode assembly (MEA).

The anode catalyst layer is a platinum/carbon-dispersed ink similarly coated on a carbon-paper gas diffusion layer. The anode catalyst platinum loading is between 0.3 and 0.4 mg Pt cm^{-2}. Gaskets are selected for 25–30% compression on both the anode and the cathode. Using a static press, the anode and cathode catalysts are bonded to a pair of cast Nafion® membranes (each 30-μm thick, 1000 EW) at ~135 °C for 10 min. The resulting MEA is tested in a standard 50-cm^2 fuel cell test fixture with quad serpentine flow fields (from Fuel Cell Technologies).

2.3. Electrochemical and fuel cell testing

Using the 50-cm^2 test cell described above, cyclic voltammograms with nitrogen flowing to the cathode are obtained to provide insight about the surface of the catalyst. Polarization curves under oxygen are then recorded. The anode under hydrogen is used as a quasi-reference hydrogen electrode and all the voltages presented are the cell voltages without any corrections. Due to the relatively low current densities, the high platinum loading on the anode, and hydrogen flow rates well over stoichiometric, it is reasonable to assume that the anode voltage is close to the reversible hydrogen potential at all times. A Solarton 1470 potentiostat controlled by CorWare™ software (Scribner Associates) was used for all the testing.

3. Results and discussion

In this section we present data showing the performance of NPM catalysts derived from two nitroaniline precursors and the processing steps leading to the most active catalysts. We also present data describing the effect of catalyst loading on the key performance characteristics as well as data related to the catalyst ORR selectivity. Finally, fuel cell performance of our most active NPM catalyst will be compared with the best activity reported for similar NPMC as well as with the state-of-the-art performance of a platinum catalyst.

3.1. Precursor and processing

Initially, two nitroaniline isomers were studied to determine the most appropriate precursor for NPMC. Depicted in Fig. 2 are the cyclic voltammograms under nitrogen and polarization curves for catalysts derived from both 2- and 4-nitroaniline precursors and a mixture (1:1 mole ratio) of the two precursors. In spite of the fact that the two isomers are structurally related and that the polymers derived from these isomers are thermally treated in ammonia to high temperatures, a large difference in the electrochemical behavior is observed. Fig. 2A shows the cyclic voltammograms recorded under nitrogen. These voltammograms are the result of the double layer charging with addition of the charge related to the presence of surface redox groups. All three voltammograms are rather featureless except for the slightly pronounced peaks between 0.57 and 0.59 V coinciding with voltage for the quinone–hydroquinone redox couple. Assuming that similar surface species are present, the integrated area (charge) of the cyclic voltammograms can be taken as a relative measure of surface area. Using this approach, the surface area of the catalyst derived from 2-nitroaniline is about half that of to 4-nitroaniline-derived material.

Fig. 2B shows the catalytic activity of the nitroaniline-derived catalyst materials. It can be seen that the catalysts' activity in the kinetic region is even more dependent on the precursor isomer. At the relatively small current density of 1 mA cm^{-2}, the catalyst

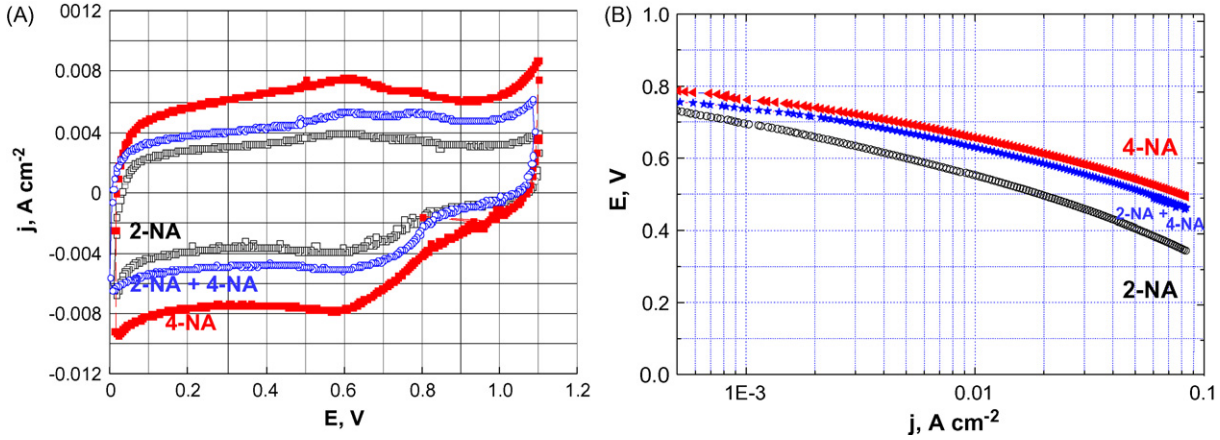

Fig. 2. (A) Cyclic voltammograms characterizing the catalysts made from 2-nitroaniline, 4-nitroaniline and a combination of 2- and 4-nitroaniline precursors. CVs are taken at 50 mV s^{-1} under hydrogen/nitrogen at 75 °C with 132% RH. (B) Polarizations curves of the catalysts in (A) measured at 80 °C with saturated hydrogen (180 sccm) and oxygen (335 sccm) with 300 kPa backpressure on anode and 430 kPa backpressure on cathode. Voltage scan rate: 5 mV s^{-1}.

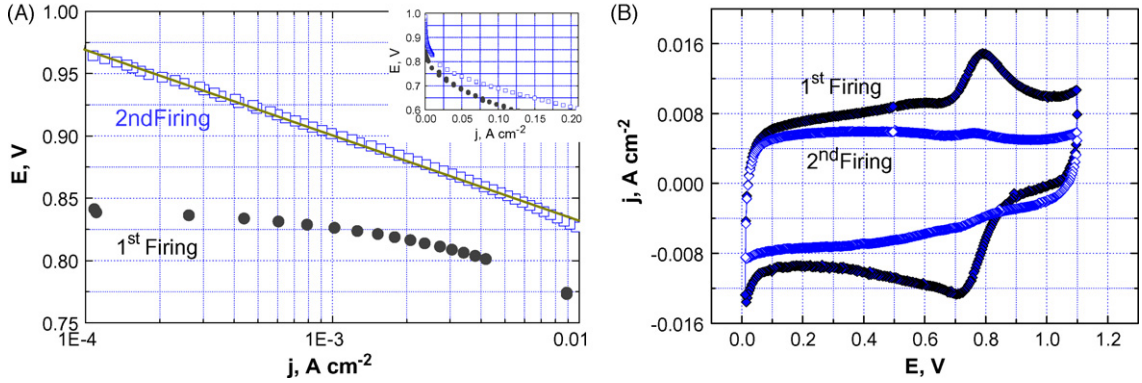

Fig. 3. (A) Polarization curves of the 4-nitroaniline precursor-based catalyst after the first firing (circles) and after the second firing (squares); test conditions are the same as in Fig. 2B. The straight-line slope is 70 mV decade^{-1}. Inset: polarization curves on a linear scale. (B) Cyclic voltammograms of the catalysts in (A); test conditions are the same as in Fig. 2A.

derived from 4-nitroaniline is more active by about 70 mV, indicating possibly even an order of magnitude higher activity than for the 2-nitroaniline-derived catalyst. Both the surface area and the catalytic activity of the material made from the mixture of the two isomers fall in between that measured for catalysts derived from each precursor separately as if each precursor has kept its own features, i.e. as if their properties are additive. These observations provide a notable example of where small changes in the structure of a precursor molecule produce marked differences in the electrochemical properties of the resulting catalysts despite the fact that the catalysts are derived from a high temperature pyrolysis in a reactive gas.

After establishing that 4-nitroaniline is the precursor of choice, a variety of modifications in the synthetic procedure were evaluated in order to determine their effect on catalyst activity. The most beneficial is the additional firing step after the milling of the catalyst (step (d) in Section 2.1). This step increases fuel cell performance 30 mV to over 100 mV throughout the polarization curves. The difference is most pronounced in the kinetic region as illustrated in Fig. 3A. The second firing generates a catalyst that under the applied testing conditions produces extremely high catalytic activity with ORR starting at unusually high voltage of 0.97 V. This activity is maintained throughout a large linear Tafel region extending over two decades, with a slope of 70 mV decade^{-1}.

From practical point of view, the fuel cell performance of the best performing catalysts can be better appreciated by observing the full polarization curves shown on a linear scale, see the inset in Fig. 3A. The fuel cell performance is recorded for voltages that are above 0.6 V, a range that is useful for energy efficient FC operation.

Simultaneously with the increased catalytic activity, the second heating step decreases the iron content in the catalyst. Even though also washed in acid, the catalysts after the first firing very often exhibit a redox peak at approximately 0.78 V that can clearly be ascribed to ferrous–ferric redox couple due to the presence of iron as a remnant from the polymerization of the nitroaniline. The Fe^{2+}/Fe^{3+} peaks are persistent throughout the performance testing in the fuel cell, which usually takes between 3 and 7 days, indicating that the iron is in a form that is not readily soluble in the PEM FC environment. After the second firing at 800–1000 °C, in most cases the redox peaks disappear (Fig. 3B). Since the second firing step takes place after the milling, it can be assumed that more iron, which during the first firing is probably "blocked" within the polymer, is accessible to the gasses flowing during the heat treatment. As a result, more iron is accessible for dissolution during the acid washing step (e) leading to lower iron content in the finished catalyst. In the group of highest performing catalysts, the estimated amount of iron in the catalyst layer as determined by X-ray fluorescence is between 4 and 12 μg cm^{-2} of geometric area of the fuel cell.

3.2. Catalyst loading and selectivity

Since the cost of NPMC is not prohibitive, we have explored the effect of higher catalyst loading on the FC performance. For this purpose, fuel cells with different catalyst loadings (approximately 1, 2 and 2.8 mg cm^{-2}) were prepared and tested. Because the exact nature of the active sites is unknown, catalyst loading refers to the total mass of powder upon which the catalyst was deposited per geometric area.

Although the current at a given voltage increases with loading, there is not a 1:1 relationship. To gain insight into the relationship between catalyst loading and fuel cell performance, we have also examined the dependence of the surface area and the durability of NPM catalyst on the loading. Fig. 4 shows the cyclic voltammograms recorded under nitrogen for the three different catalyst loadings. The voltammograms exhibit the same features for all the loadings and the current responses seem to be proportional to the catalyst loading. Because the catalyst for all three FCs has come from the same batch, a comparison of the charge of the CVs gives a measure of the relative surface area. Fig. 5 shows the values for the surface area normalized to the lowest loading and that the proportionality factor is less than one, 0.89. This could indicate that there might be some agglomeration in the thicker catalyst layers. Fig. 5 also shows that catalyst performance increases by only 0.68 as the loading is increased. While the reasons for these findings were not explored further, a different ratio of catalyst to ionomer in the catalyst ink might be required in order to avoid agglomera-

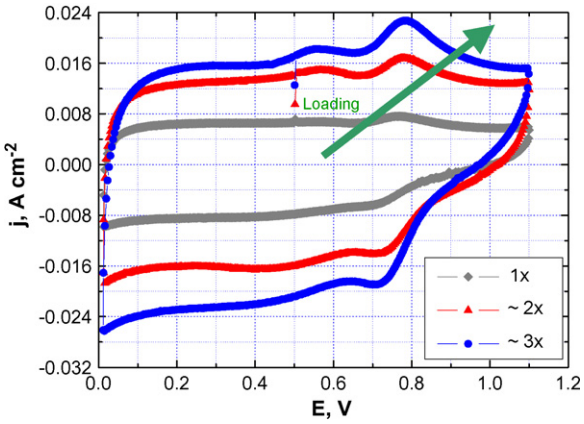

Fig. 4. Cyclic voltammograms showing the effect of catalyst loading on surface area: "1x" catalyst loading is approximately 1 mg cm^{-2}; "2x" is approximately 2 mg cm^{-2}; "3x" is approximately 2.8 mg cm^{-2}. CVs taken under the same conditions as in Fig. 2A.

tion and to access all the catalyst sites in the thicker catalyst layer.

The most interesting dependence on the catalyst loading presented in Fig. 5 is durability. The normalization for the durability was done with respect to the initial performance of each of the fuel cells tested. In the first 40 h of continuous operation the cell with a catalyst loading of 1 mg cm^{-2} loses two-thirds of its original performance. This finding is typical of the samples that were tested. It is generally accepted that the generation of peroxide is the most probable cause for the loss of performance in NPM catalysts [3]. Rotating ring-disk electrode (RRDE) testing of our catalyst showed a rather substantial amount of peroxide, approximately 10%. In order to explain the improved stability with a thicker catalyst layer, two things can be considered. First, at a given voltage, the volumetric current density for the thicker catalyst layer is lower since

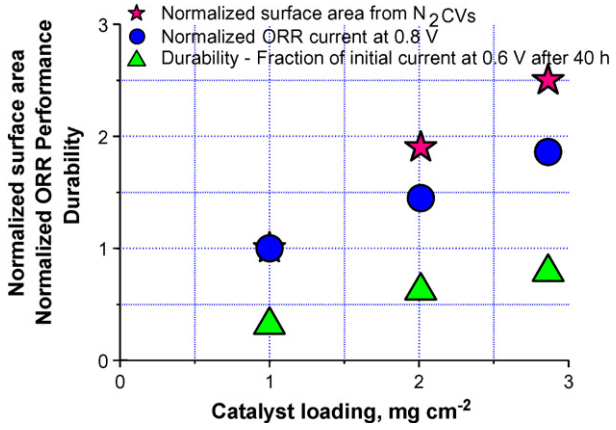

Fig. 5. Three normalized FC properties, surface area, ORR current, and durability, in relation to loading of the 4-nitroaniline-derived catalyst. Surface area (stars) assessed from CVs in Fig. 4 and normalized to the value for 1 mg cm^{-2} catalyst loading; ORR performance is the current at 0.8 V (circles) normalized to the value for 1 mg cm^{-2} catalyst loading under the conditions noted in Fig. 2B; durability (triangles) represents the fraction of the initial ORR performance after 40 h running potentiostatically at 0.6 V at 75 °C with saturated hydrogen and air at approximately 300 kPa backpressure on both anode and cathode.

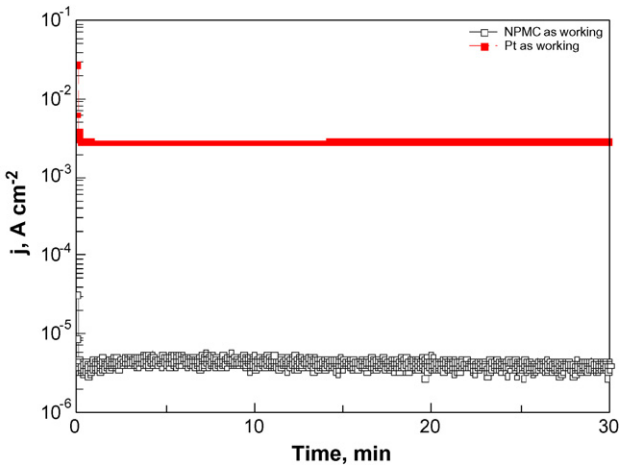

Fig. 6. NPM catalyst response to hydrogen cross-over. Fuel cell at 80 °C, 300 kPa/430 kPa backpressure, 180 sccm hydrogen/335 sccm nitrogen, saturated gas streams, at 0.6 V potentiostatic hold. The cell is first run with nitrogen on the NPM catalyst side of the cell (hydrogen on Pt side) and then reversed (both gases and polarity), with nitrogen on the Pt catalyst side of cell (hydrogen on NPM catalyst side).

the current increase with the catalyst loading is by a factor of 0.68. Therefore, the concentration of peroxide in the catalyst layer should be smaller. However, this concentration is still relatively high compared to that measured for a platinum-based catalyst.

Second, recent platinum loading RRDE studies provide another possible explanation for increased durability. Studies showed that the amount of peroxide formed is related to the amount of the catalyst deposited on the disk; the amount of peroxide decreases as the amount of catalyst on the disk increases [14,15]. In a thicker catalyst layer the peroxide generated during the ORR has more opportunities to be further reduced or decompose to water, thus decreasing the chances of the peroxide attacking the catalytically active sites.

The selectivity of the catalyst towards ORR plays an important role in the performance of a fuel cell. In a hydrogen–oxygen (air) fuel cell, the gasses from one electrode can diffuse through the membrane to the other electrode area (cross-over effect) lowering the performance of the respective electrodes. Since this NMPC is meant to be used on the cathode side, it is of interest to know what would be the reactivity of hydrogen diffusing through the membrane on this catalyst. A fuel cell with the usual construction, NPMC on the cathode and platinum on the anode side, was run with hydrogen on the anode and nitrogen on the cathode side. The voltage is potentiostatically controlled at 0.6 V and the current response is measured. For comparison purposes, the polarity of the imposed voltage and the gasses are reversed. The current due to the oxidation of hydrogen crossing over is presented in Fig. 6. Since at 0.6 V hydrogen is almost completely oxidized when it reaches platinum, three orders of magnitude lower current is observed when nitrogen is flowing over NPMC. This indicates that nitroaniline-derived NPMCs are very selective in a PEM FC, i.e. active only for ORR.

3.3. Catalytic activity comparison

Among the many NPM catalysts with similar final compositions, mostly carbon, some nitrogen and much less Fe, the ORR activity of these catalysts can vary significantly depending on the precursors and the synthesis methods. We will compare the activity of the nitroaniline-derived catalyst with the best performance of a recently published NPM catalyst in the C–N–Fe category from Dodelet's group [16]. The current densities in the catalytic region are over three times higher for the nitroaniline-derived catalyst than that measured by Ruggeri and Dodelet: 32 mA cm^{-2} (see Fig. 3A) vs. 10 mA cm^{-2} [16] at 0.8 V. It is important to point out that the fuel cell testing conditions, with the exception of the fuel cell size (1.13 cm^2 vs. 50 cm^2), used by Dodelet's group and in this work are very similar: the temperature (80 °C) is the same and the relative humidity and oxygen partial pressure are similar. In addition, the amount of catalyst used is also approximately the same, 1 mg cm^{-2}. In order to explain the difference in the catalytic activity, we will look next to the composition of the two catalysts.

Dodelet's group has proposed that the limiting step in the creation of the catalytically active sites is the small concentration of surface pyridinic nitrogen as coordination sites for the iron. Therefore, it is instructive to compare the nitrogen and iron contents in these two materials. The approximately 6 μg iron cm^{-2} in our highest performing catalyst is the same as reported by Dodelet's group for their most active catalyst [16]. The major difference in the composition of the catalysts is the content of the surface nitrogen, which at 4% for the nitroaniline-derived catalyst is almost by a factor of two higher than the highest ever reported by Dodelet's group. The same is true for the XPS N 1s component with a binding energy of ~398.5 eV, assigned as pyridinic by Dodelet's group [3,4], which accounts for ~32% of the nitrogen for both catalysts (for possible assignments of the 398.5 eV binding energy to functionalities different than pyridinic nitrogen, see [9,10]). Clearly, these two Fe-derived catalyst materials contain different amounts of total surface nitrogen as well as the 398.5 eV nitrogen component. Since the amount of iron in both materials is about the same but the activity differs, one may ask if catalytically active sites exist that do not contain iron. Indeed, it was recently proposed that nitrogen-rich carbon with no detectable transition metal at the surface can be very active for ORR in PEM fuel cells [17].

The main goal of this NPMC synthesis project was to achieve DOE performance targets for volumetric current density, which measured at 0.8 V under hydrogen–oxygen are 130 A cm^{-3} for year 2010 and 300 A cm^{-3} in 2015. Fig. 7 compares the polarization curve of the most active nitroaniline-derived NPM catalyst, as presented in Fig. 3A, with a state-of-the-art platinum catalyst [12]. Comparisons of NPMC catalysts with platinum are frequently uninformative because they are done with an inferior-performing Pt-based fuel cell. In contrast, the comparison presented here is more credible for several reasons. Our data is obtained from a 50 cm^2 fuel cell, an accepted test standard. Second, the calculated volumetric current density is based on the measured thickness of the coated catalyst layer. Finally, the platinum data used in the comparison was obtained from an independent source.

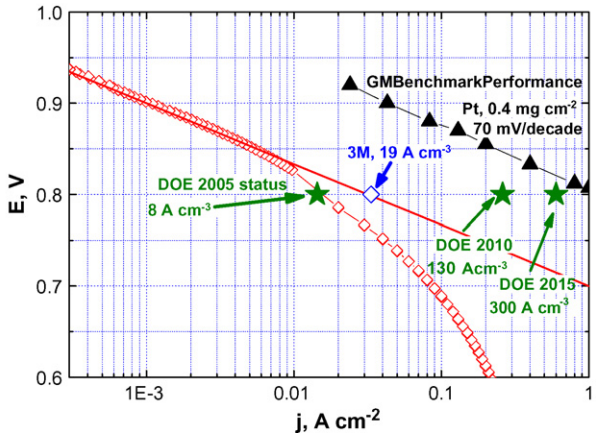

Fig. 7. Polarization curves comparing of highest activity NPM catalyst to platinum and DOE targets. Both tests under hydrogen–oxygen at 80 °C, 100% relative humidity. Oxygen pressure: 430 kPa for 3M catalyst and 150 kPa for GM Pt. Detailed test conditions: 3M catalyst as in Fig. 3B; GM Pt as in refs. [12,13].

From electrochemical point of view this particular comparison can be seen to be valid because the two curves have the same Tafel slope allowing comparison at any current density or voltage. The extended linear Tafel region on the NPMC allows the inherent activity of the catalyst to be revealed by accurate extrapolation that encompasses all the necessary corrections for IR drop and diffusion polarization. Although the catalyst activity reported here is still far from the performance attained using platinum, the activity of the 4-nitroaniline-derived NPM catalyst, 19 A cm^{-3} at 0.8 V, is only a factor of seven lower than the DOE 2010 goal of 130 A cm^{-3}. We believe that with further research, partly by optimization of the catalyst ink but mostly by improving the inherent catalytic activity, this class of catalyst materials may approach US DOE performance goals.

4. Conclusion

In summary, a highly active ORR NPM catalyst based on a new precursor, 4-nitroaniline, has been synthesized and characterized. Catalysts based on this material show unusually high ORR onset voltages, above 0.9 V, and Tafel slopes of 70 mV decade^{-1}. We believe that with further process improvements catalyst performance can be increased and that by substituting the carbon support we will obtain a more durable 4-nitroaniline-derived catalyst, one that shows promise to achieve the near-term goals as a substitute for platinum. In addition, since the price of nitroaniline on the commodity market is around \$1.5 kg^{-1}, the criterion for a catalyst to be acceptable for a large-scale application, its cost, is also satisfied. A potential drawback in developing a process based on nitroaniline could be its high toxicity. For this reason, we are in the process of developing new, non-toxic analogs for inexpensive and safe NPMC production.

Acknowledgments

The contributions of the non-precious metal catalyst team at 3M, Manish Jain, Dennis O'Brien, George Vernstrom, Shih-Hung Chou, Judith Hartmann, Michael Kurkowski, and Allen Siedle in particular, to a variety of aspects of this paper are acknowledged. As a part of the same team, the contributions of Prof. Jeff Dahn's group at Dalhousie University, specifically peroxide measurements by Arman Bonakdarpour and the critical review of this manuscript by Jeff Dahn are also acknowledged.

This work was supported by the U.S. Department of Energy (DOE), Cooperative Agreement No. DE-FC36-03GO13106. DOE support does not constitute an endorsement by DOE of the views expressed in this article.

References

[1] C.H. Paik, T.D. Jarvi, W.E. O'Grady, Electrochem. Solid State Lett. 7 (2004) A82.
[2] H. Xu, H.R. Kunz, J.M. Fenton, Electrochem. Solid State Lett. 10 (2007) B1.
[3] J.P. Dodelet, in: J. Zagal, F. Bedioui, J.P. Dodelet (Eds.), N_4-Macrocyclic Metal Complexes (Ch. 3), Springer Science, Business Media Inc., 2006.
[4] M. Lefevre, J.P. Dodelet, J. Phys. Chem. B 104 (2000) 11238;
F. Jaouen, S. Marcotte, J.P. Dodelet, G. Lindbergh, J. Phys. Chem. B 107 (2003) 1376.
[5] F. Jaouen, J.P. Dodelet, J. Phys. Chem. B 111 (2007) 5970.
[6] R. Atanasoski, Novel Approach to Non-Precious Metal Catalysts, DOE Hydrogen Program Annual Progress Reports: FY 2003, IV-253; FY 2004, IV.C.5, p. 392. Available online at: http://www1.eere.energy.gov/hydrogenandfuelcells/annual_reports.html.
[7] E.B. Easton, A. Bonakdarpour, R. Yang, D.A. Stevens, D.G. O'Neill, G. Vernstrom, D.P. O'Brien, A.K. Schmoeckel, T.E. Wood, R.T. Atanasoski, J.R. Dahn, ECS Trans. 3 (1) (2006) 241.
[8] D.G. O'Neill, R. Atanasoski, A.K. Schmoeckel, G.D. Vernstrom, D.P. O'Brien, M. Jain, T.E. Wood, Mater. Matter 1 (3) (2006) 17.
[9] See ref. [9] for web access, FY 2005, VII.C.9, p. 854.
[10] See ref. [9] for web access, FY 2006, V.C.9, p. 805.
[11] L.A. Errede, R.A. Sinclair, S. Newman, React. Polym. Ion Exch. Sorbents 8 (1988) 201.
[12] H.A. Gasteiger, S.S. Kocha, B. Sompalli, F.T. Wagner, Appl. Catal. B: Environ. 56 (2005) 9.
[13] DOE Multi-Year Research, Development, and Demonstration Plan, available on DOE Hydrogen Fuel Cell Program at: http://www1.eere.energy.gov/hydrogenandfuelcells/mypp/.
[14] M. Inaba, H. Yamada, J. Tokunaga, A. Tasaka, Electrochem. Solid State Lett. 7 (2004) A474.
[15] A. Bonakdarpour, K. Stevens, G.D. Vernstrom, R. Atanasoski, A.K. Schmoeckel, M.K. Debe, J.R. Dahn, Electrochim. Acta 53 (2007) 688.
[16] S. Ruggeri, J.P. Dodelet, J. Electrochem. Soc. 154 (2007) B761.
[17] V. Nallathambi, G. Wu, N.P. Subramanian, S.P. Kumaraguru, J.-W. Lee, B.N. Popov, Proceedings of the 212 Meeting of the Electrochem. Soc., Washington, DC, October 2007 (Abstract #585).